CFD model to evaluate the performance of a low-rise building exposed to hurricane wind loads with different configurations.

Jonathan Francisco Gutiérrez Guzmán, Dr. Jaime Moisés Horta Rangel, Dr. Miguel Ángel Pérez Lara y Hernández
Faculty of Engineering
Universidad Autónoma de Querétaro
Santiago de Querétaro, México
pacogutierrezguzman@outlook.es

Dr. Humberto Yáñez Godoy
Institute of Mechanical Engineering (I2M)
University of Bordeaux
Talence, France
humberto.yanez-godoy@u-bordeaux.fr

***Abstract*— This paper is the second stage of a scientific investigation that presented a review of mitigation strategies in coastal areas. In order to evaluate parameters of interest for the design of low-rise buildings, such as pressure coefficients, C_p, and wind behavior around the structure, 36 configurations based on a Central Composite Design (CCD) were simulated using Computational Fluid Dynamics (CFD) with a RNG $k-\epsilon$ turbulence model. The results in terms of wind velocity and behavior, as well as turbulence kinetic energy, were validated with respect to the existing literature, obtaining similar and acceptable contours, streamlines and vectors. These results showed that the negative values of C_p and velocity are more important, i.e., the suction effects have a greater impact on the building than the overpressure effects. By elevating the structure, the wind behavior around it causes vorticity, which in turn leads to negative pressures, especially on the roofs, lower floor and downstream walls. The results obtained should allow: (1) to generate a predictive model based on the C_p coefficients using the Response Surface Methodology (SRM) and (2) to propose mitigation strategies against hurricane winds.**

Keywords—Computational Fluid Dynamics; Low-rise building; Central Composite Design; RNG $k-\epsilon$ turbulence model.

I INTRODUCTION

The use of Computational Fluid Dynamics (CFD) has grown enormously in recent years, thanks to computational advances. Many researchers around the world use this tool as an alternative in the study of flow behavior through a domain. This methodology allows optimizing time and costs, standing out from other methodologies such as the use of the wind tunnel and full-scale experimentation.

In the scientific engineering sector, CFD simulation is an ally to develop research in different areas, particularly in fluid-structure interaction, however, a topic that is vital today for Mexico and the world population are mitigation strategies for low-rise structures in the face of extreme winds such as those generated by hurricanes since in past events they have left great economic and human losses [1], [2], and they are expected to be more frequent and intense [3], [4].

This work aims at evaluating the pressure coefficient C_p and the wind behavior for low-rise structures. Different configurations are considered using CFD methodology. Central Composite Design (CCD) method, [5] [6] [7] [8], were used to create the different combinations by knowing the significant factors from the literature. For this purpose, ANSYS FLUENT 2022 R2 was used with a Re-Normalisation Group k-epsilon turbulence model (RNG $k-\epsilon$) described later.

II BACKGROUNDS

Several authors have carried out research using CFD simulations to investigate the behavior and mitigation strategies that allow dissipating the effects caused by wind loads. In [5], one- story and two-story gable roof models with different elevations were presented to determine the effects in different parts of the house. The study presented by [6] showed that different configurations provided a better understanding of the behavior of elevated houses, recommending the continuity of more variables and mitigation techniques to improve stability against wind pressures. In [8], the pressure distribution around gable roof with different roof pitches and wind directions were investigated. In [9], pyramidal roof presented a better aerodynamic behavior compared to different roof geometries. In [10], the optimal roof/solar panel combination reduced wind loads on low-rise buildings. In [11], different configurations with various edges were explored, highlighting the proposal of an aerodynamic edge inspired by airplane wings to help reduce wind loads. This also helps to interrupt vortex formation and divert the flow from the clearance zone on the roof edge away from weak elements. Something similar was presented in [12], where corner cut- shaped modifications were analyzed.

III MATERIALS AND METHODS

A. *Central composite design, CCD*

CCD was used to explore 5 factors at 5 levels. Table 1 gives the factors and levels used, and Fig.1 shows the input factors for building configurations. It is known from the literature that these factors are significant in the C_p and flow behavior results. Equation 1 was used to determine the number of simulations performed:

$$N = 2^{k-1} + 2k + n_0 \quad (1)$$

Where k=5 and n_0 = 10. MATLAB software was used to determine the different configurations showed in Table 3.

Table 1 Factors and levels for the CCD.

Input	Level -2	Level -1	Level 0	Level 1	Level 2
Wind angle, θ(°)	0	45	45	45	90
Roof slope, α (°)	3	10	20	30	35
Building opening, %	0	15	20	25	30
Ratio, L/b	0.5	1	1.5	2	2.5
Height of pile above ground, h (m)	0	1.5	2.5	3	3.5

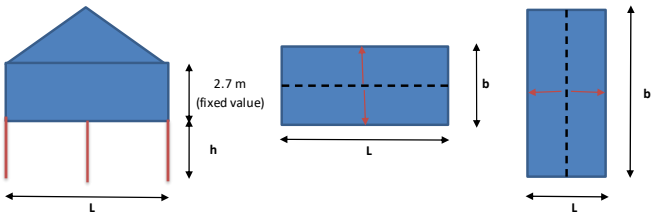

Fig. 1 Input factors for building configurations.

B. *CFD model*

The process that was used to carry out the 36 CFD configurations (Table 3) consists of 3 steps: (1) Pre-processing: geometries, meshing and simulations configurations were defined; (2) Processing: solution was calculated; (3) Post-processing: analysis of results. The scale used for each simulation was 1:20, as used by [6]. All the recommendations presented in the literature were considered to obtain reliable results such as [5], [8], [13]. The L/b ratio is described in Table 2 considering important characteristics such as the minimum construction square meters considered by the Mexican regulations, as well as an average static height of 2.7 m at the eaves level.

Table 2 Values of L and b corresponding to the building side.

Units in meters at full scale			
L	b	Ratio L/b	Area (m^2)
5	10	0.5	50
8	8	1	64
8	5.3	1.5	42.4
10	5	2	50
13	5.2	2.5	67.6

C. *Governing equations and boundary conditions*

ANSYS WORKBECH FLUENT 2022 R2 was used in this study to perform the steady Reynolds-Averaged Navier-Stokes (RANS) computations. RANS allows to solve the mean flow model fluctuations. The building models were created based on the dimensions given by CCD. The software helped to solve the Navier-Stokes equations by Finite Volume Method (FVM), the pressure and momentum equations are coupled using the SIMPLE algorithm presented in [14]. The Navier-Stokes equations describe the physical characteristics of the flow. This is a system of five partial differential equations, which for a Newtonian, incompressible and isothermal fluid in steady-state, are simplified in the form of continuity and momentum equations [1]:

$$\frac{\partial u_i}{\partial x_i} = 0 \quad (2)$$

$$u_j \frac{\partial u_i}{\partial x_j} = -\frac{1}{\rho}\frac{\partial p}{\partial x_i} + v\frac{\delta^2 u_i}{\delta x_j \delta x_j} \quad (3)$$

Where v is the kinematic viscosity, defined as viscosity (μ), divided by the density (ρ).

The RNG $k-\epsilon$ turbulence model is considered in this study to model the Atmospheric Boundary Layer (ABL). This model consists of two additional transport equations for the Turbulence Kinetic Energy (TKE), k, and the rate of dissipation of TKE, ϵ, [15], and is expressed as:

$$\frac{\partial}{\partial z}\left(\frac{\mu_t}{\sigma_k}\frac{\partial k}{\partial z}\right) + G_k\frac{\epsilon}{k} - \rho\epsilon = 0 \quad (4)$$

$$\frac{\partial}{\partial z}\left(\frac{\mu_t}{\sigma_\epsilon}\frac{\partial k}{\partial z}\right) + C_{\epsilon 1}G_k\frac{\epsilon}{k} - C_{\epsilon 2}\rho\frac{\epsilon^2}{k} = 0 \quad (5)$$

Where the production of TKE is given by

$$G_k = \mu\left(\frac{\partial u}{\partial z}\right)^2 \quad (6)$$

Table 3 CCD configurations.

#	θ (°)	α (°)	%	L/b	h (m)	#	θ (°)	α (°)	%	L/b	h (m)
1	45	10	15	1	3	19	45	3	20	1.5	2.5
2	45	10	15	2	1.5	20	45	35	20	1.5	2.5
3	45	10	25	1	1.5	21	45	20	0	1.5	2.5
4	45	10	25	2	3	22	45	20	30	1.5	2.5
5	45	30	15	1	1.5	23	45	20	20	0.5	2.5
6	45	30	15	2	3	24	45	20	20	2.5	2.5
7	45	30	25	1	3	25	45	20	20	1.5	0
8	45	30	25	2	1.5	26	45	20	20	1.5	3.5
9	45	10	15	1	1.5	27	45	20	20	1.5	2.5
10	45	10	15	2	3	28	45	20	20	1.5	2.5
11	45	10	25	1	3	29	45	20	20	1.5	2.5
12	45	10	25	2	1.5	30	45	20	20	1.5	2.5
13	45	30	15	1	3	31	45	20	20	1.5	2.5
14	45	30	15	2	1.5	32	45	20	20	1.5	2.5
15	45	30	25	1	1.5	33	45	20	20	1.5	2.5
16	45	30	25	2	3	34	45	20	20	1.5	2.5
17	0	20	20	1.5	2.5	35	45	20	20	1.5	2.5
18	90	20	20	1.5	2.5	36	45	20	20	1.5	2.5

And the turbulence viscosity, μ_t, is given by:

$$\mu_t = \rho C_\mu \frac{k^2}{\epsilon} \quad (7)$$

σ_k, σ_ϵ, $C_{\epsilon 1}$, $C_{\epsilon 2}$ and C_μ are model constants, which are usually assigned the values 1, 1.3, 1.44, 1.92 and 0.09 respectively.

In this paper, the following equations were implemented to satisfy the above equations recommended by [15]: Eq. (8), velocity profile, u; Eq. (9), k parameter; Eq. (10), ϵ parameter.

$$u = \frac{u_*}{\kappa} ln\left(\frac{z + z_0}{z_0}\right) \quad (8)$$

$$k = \frac{u_*^2}{\sqrt{C_\mu}} \quad (9)$$

$$\epsilon = \frac{u_*^3}{\kappa\,(z + z_0)} \quad (10)$$

Where κ is von Karman's constant, z is the height in which the velocity is calculated, z_0 is the surface roughness length and u_* is the friction velocity that can be calculated as:

$$u_* = \kappa \frac{u_{ref}}{ln\frac{z_{ref} + z_0}{z_0}} \quad (11)$$

Where u_{ref} is the velocity reference, and z_{ref} is the length of the velocity reference.

One of the values of interest in this paper, is the C_p, that is a dimensionless parameter very important for the structural design of buildings and is calculated as:

$$C_p = \frac{P - P_0}{0.5\rho u_{ref}^2} \quad (12)$$

Where P = static pressure on the surface; P_0 = static pressure at the reference point, ρ = air density.

Finally, another important parameter to determine is the appropriate cell size near the walls since the wall laws of the turbulence model have constraints on the y^+ value at the wall. The following equation can be used to predict the height of the first layer:

$$y^+ = \frac{\rho * u_* * y_p}{v} \quad (13)$$

Where y_p is the distance from the center of the cell to the nearest wall.

D. Geometry

The geometries were created in ANSYS CAD SPAICE CLAIM respecting: 1:20 scale; mezzanine height of 135 mm; square piles of 15×15 mm^2 corresponding to the foundation; each window was positioned 45 mm from the floor and centered on the width of the wall as shown in Fig. 2. The height of the window was considered as a function of percentage of building opening: 50 mm for values ≤ 20% and 75 mm for values≥ 25%. Flow domain was delimited by the corresponding boundary conditions, with H = 183 mm. To reduce computing time, the minimum recommended boundary distances were used, such as [10], in Fig. 3. Each model was divided into two parts for each analysis. In addition, each of the boundary conditions (inlet, outlet, and walls) was named since the software recognizes the names for further processing.

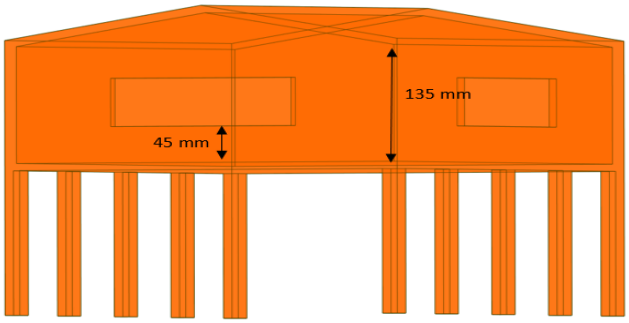

(a)

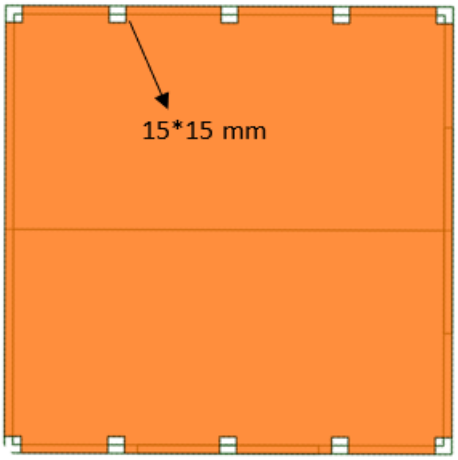

(b)

Fig. 2 Geometry: a) Fixed dimensions of each model; b) Dimensions and distance between piles (distance is equidistant trying not to exceed 100 mm of separation).

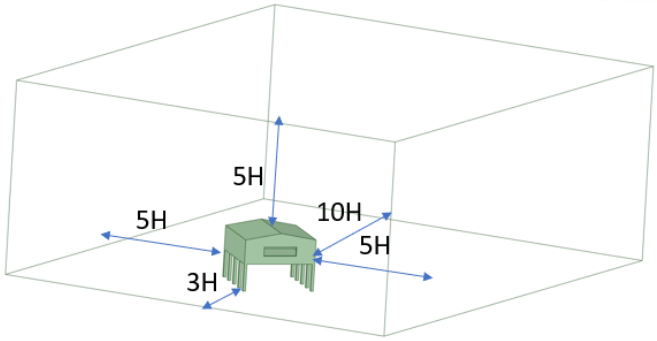

Fig. 3 Flow domain and boundary distances.

E. Meshing

Meshing was generated in ANSYS FLUENT. Each CAD model was exported considering each of the important features for the quality of the model. A mesh sensitivity analysis was performed for all cases. A fine mesh was selected for each configuration with the smallest cell of 2.5 mm in the house walls. In addition, each scenario presents a combination of polyhedral cells using the Poly-Hexacore tool [16] (Fig. 4). Each configuration in Table 3 is between the order of 3,000,000 and 5,000,000 of cells. For the walls of the house, 10 layers were used with the thickness of the first layer of 0.6 mm and a transition ratio of 0.272, Therefore, the averaged of $y^+ < 5$ for all cases. Finally, the configurations of all the meshes were checked for various factors such as maximum orthogonality and skewness.

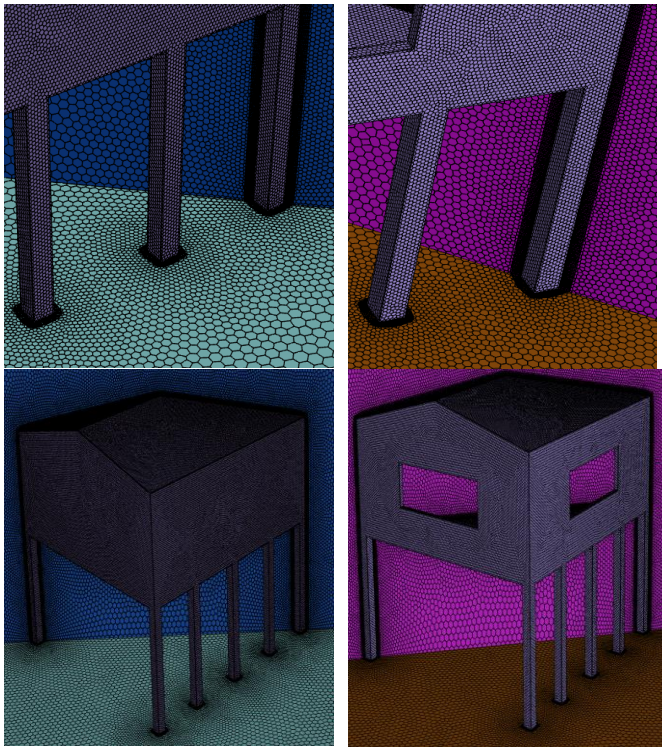

Fig. 4 Meshing used for the study.

F. Configuration and solution

All simulations were performed on a personal computer with an Intel(R) Core(TM) i7-8750H CPU @ 2.21 GHz processor and 16.0 GB RAM. Due to computing limitations, double precision and six processors were used for the simulations. Turbulence model RNG $k-\epsilon$ was selected with σ_k = 1.11. The initial values selected were gravity = 9.81 m/s^2, and the flow characteristics, density $\rho = 1.255$ kg/m^3 and viscosity $v = 0.000017894$ kg/(m·s). The inlet values for boundary conditions, in particular the wind velocity profile, were calculated using an algorithm made in C++ language with the equations (8, 9,10 and 11) and with following values: u_{ref} = 8.5 m/s; C_μ= 0.09; κ = 0.4; z_{ref} = 0.135 m and z_0 = 0.0003 m. Fig. 5 show the wind velocity profile. Zero static pressure is used on the domain outlet, and zero normal velocity and zero normal gradients of all variables are on the top and lateral sides. The house surfaces are treated as a non-slip wall subject to shear stress. The pressure and momentum equations are coupled using the SIMPLE algorithm. The discretization schemes used for the convection and diffusion terms (pressure, momentum, TKE, ϵ) are second-order upwind schemes. Convergence is achieved when all the scaled residuals are less than 1*10^{-5} (Fig 6).

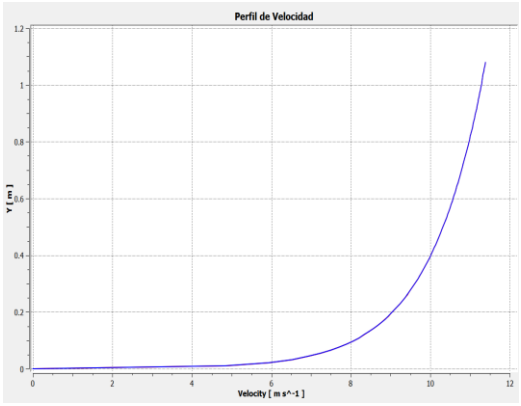

Fig. 5 Wind velocity profile used for the simulations.

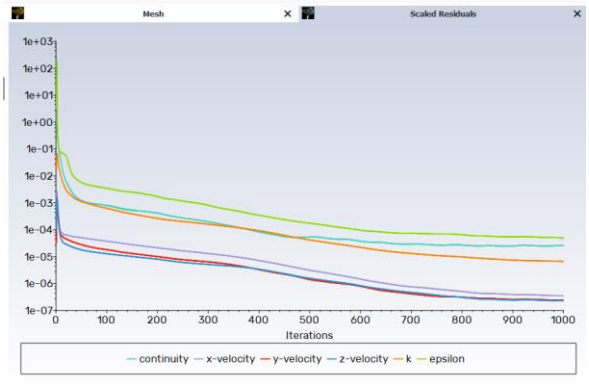

Fig. 6 Scaled residuals plot.

II. DISSCUTIONS AND RESULTS

The CFD post-processing yielded the C_p and wind velocity results shown in Table 4. To verify the results, all the factors recommended by the good practice guides were considered [13]. For the validation, the existing literature was used since due to the lack of information, it is necessary to compare with experimentation or, in this case, with similar studies. There were some differences due to the current configuration, however, it is shown in Figures 7, 8 and 9 similar results to those obtained by [5], [6], [8] and [7]. Velocity (contours, streamlines and vectors) and the TKE contours in configurations number 17, 18 and 25 were selected for comparison with the literature. The obtained results show that the negative values of C_p and velocity are more important, which means that the suction effects have a greater impact on the building than the overpressure effects. By elevating the structure, the wind behavior around it causes vorticity, which in turn causes negative pressures, especially on the roofs, lower floor and downstream walls (Figures 7a, 8a, 9a).

Table 4 Results of the C_p and wind velocity values.

# Simulation	C_p Values		Velocity Values (m/s)	
	Min	Max	Min	Max
1	-3.96734	1.65079	-4.25	12.57
2	-3.96615	1.3945	-4.28	12.35
3	-3.51461	1.41952	-5.09	12.42
4	-5.27917	1.6053	-6.29	13.63
5	-2.62301	1.59208	-5.96	13.04
6	-3.52491	1.67406	-5.36	13.65
7	-2.72515	1.74649	-5.59	13.49
8	-3.20831	1.42484	-4.47	13.05
9	-3.49846	1.4362	-5.39	12.08
10	-5.783	1.67973	-5.19	14.25
11	-3.78578	1.64995	-3.80	12.51
12	-4.32101	1.38949	-6.11	12.48
13	-2.89798	1.9072	-4.76	13.73
14	-3.548	1.54672	-5.44	13.24
15	-2.67538	1.59032	-6.37	13.17
16	-3.66177	1.70496	-4.75	13.70
17	-2.73507	1.54373	-2.69	11.54
18	-2.0292	1.50667	-3.27	11.66
19	-6.50004	1.55127	-4.53	14.72
20	-4.92323	1.70331	-5.15	15.52
21	-3.50098	1.58285	-4.88	13.20
22	-3.6075	1.58285	-5.61	13.15
23	-4.36163	1.59513	-4.18	13.02
24	-4.1635	1.57618	-4.22	12.57
25	-2.60452	1.17963	-4.38	11.87
26	-3.75827	1.70324	-4.39	13.51
27-36	-3.49029	1.58318	-5.31	13.37

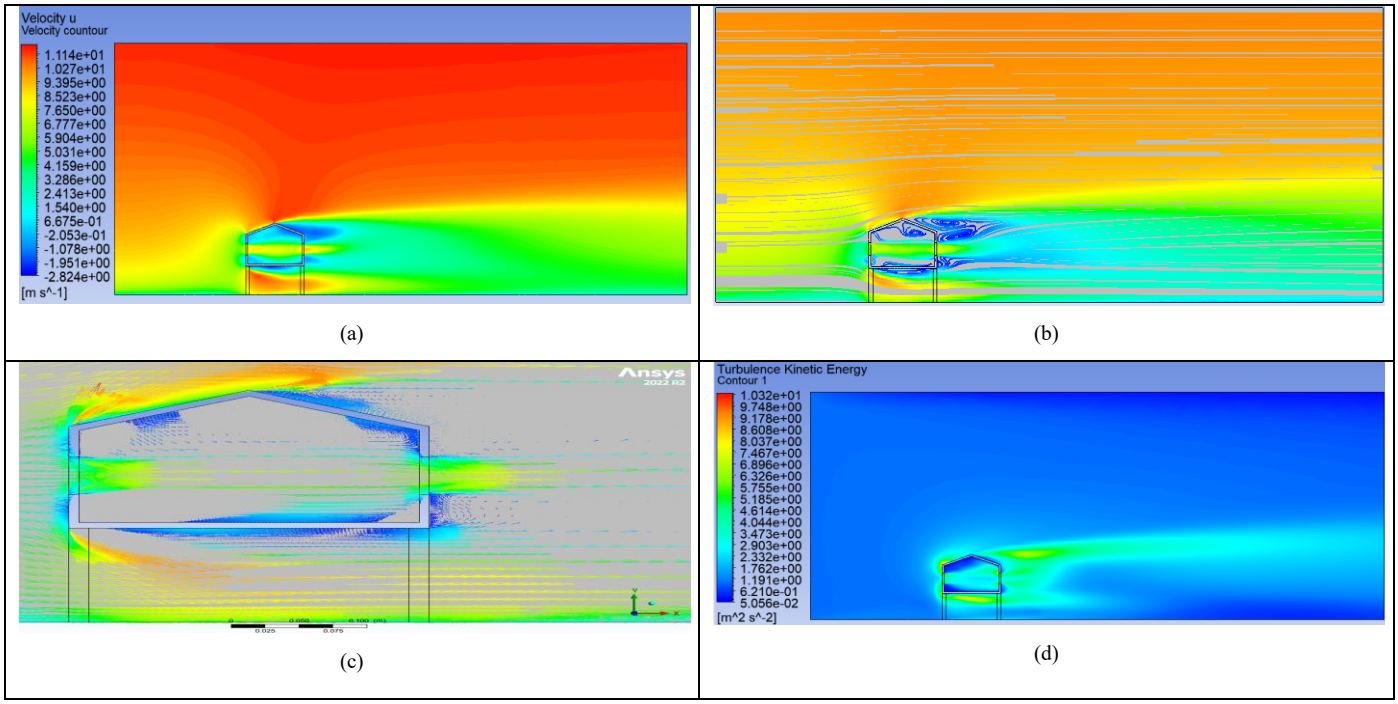

Fig. 7 Simulation 17: a) Velocity contour; b) Streamline contour; c) Vectors contour; d) TKE contour.

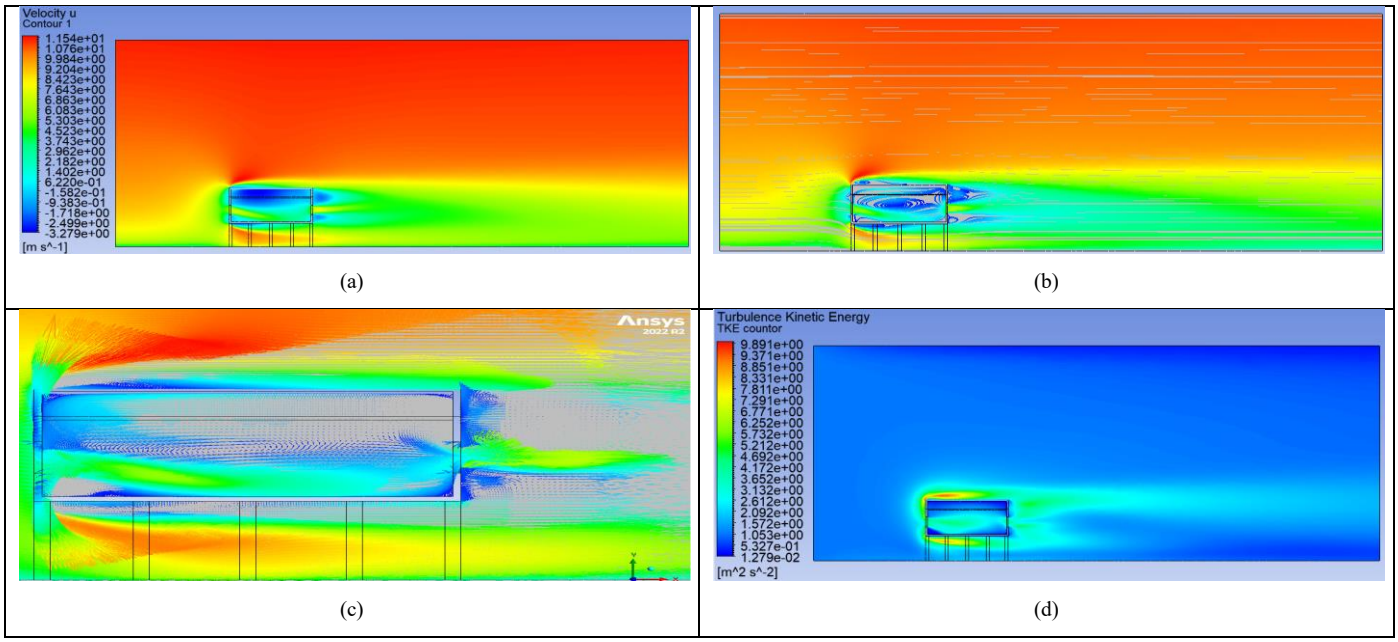

Fig. 8 Simulation 18: a) Velocity contour; b) Streamline contour; c) Vectors contour; d) TKE contour.

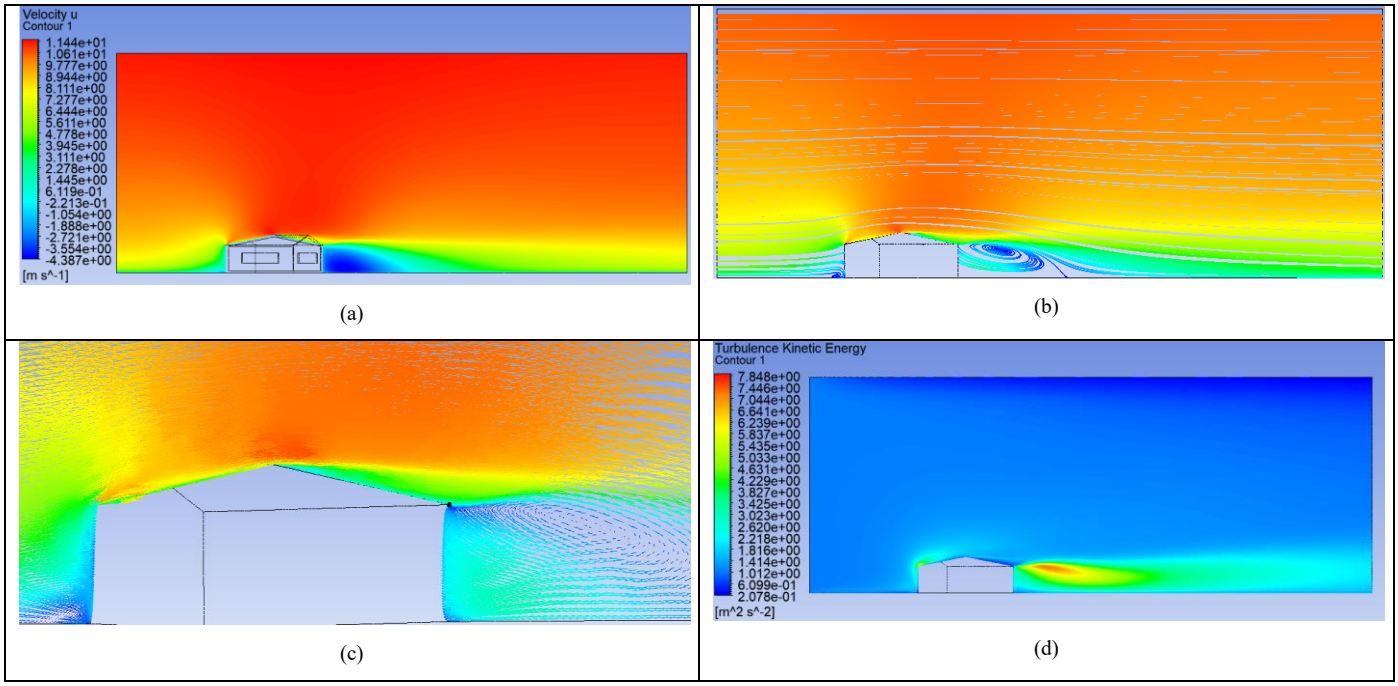

Fig. 9 Simulation 25: a) Velocity contour; b) Streamline contour; c) Vectors contour; d) TKE contour.

III. Conclusion

This study evaluated the behavior of a low-rise structure with different configurations in the face of hurricane winds in terms of pressure coefficients C_p and wind velocity. Five factors were chosen, after an exhaustive review of the literature, which have a high impact on flow behavior. Wind angle, roof slope, building opening, ratio of length to width of the structure, and height of pile above ground, were the factors selected for this project, with 5 different levels for each factor. A central composite design was used for two important purposes: (1) to significantly reduce the number of simulations, without losing valuable information and (2) to implement a predictive model.

Due to the size limitation of the paper, this work focused on two important points: obtaining accurate and reliable results in terms of C_p, wind velocity and TKE through the use of computational fluid dynamics using ANSYS FLUENT, with a turbulence RNG k-e model; and validating the obtained results by comparison with those of other authors.

Future work should consider to develop: a predictive model with response surface method or machine learning methodology; mitigation proposals to dissipate wind effects on low-rise structures; testing with a larger number of factors and levels; using other turbulence models to serve as a comparison framework; extension of the work to a set of several buildings to examine the effect of wind between neighboring structures.

Although the use of CFD saves time and money in terms of experimental facilities, it requires a high computational cost. Therefore, it is necessary to compare the results of this study by improving, for example, the level of residuals, meshing or by implementing other turbulence models that require a much higher computational cost to be performed.

Acknowledgment

The authors thank the Consejo Nacional de Ciencia y Tecnología (CONACYT), the Universidad Autónoma de Querétaro UAQ, the University of Bordeaux and the Institute of Mechanical Engineering (I2M) for the realization of this project.

References

[1] M. Rosengaus Moshinsky y J. Sánchez Sesma, «Gilbert: example of a high intensity hurricane; Gilbert: ejemplo de huracanes de gran intensidad.,» Instituto Mexicano de Tecnología del agua, CNA., p. 23, 1990.

[2] D. Murià-Vila, M. Jaimes, A. Pozos-Estrada, A. López, E. Reinoso y M. M. Chávez, «Effects of hurricane Odile on the infrastructure of Baja California Sur, Mexico,» Natural Hazards, p. 19, 2018.

[3] T. IhI y F. Martínez, «Climate change and hurricanes in the Yucatan Peninsula; El cambio climático y los huracanes en la Península de Yucatán,» Monitoreo de riesgo y desastre asociado a fenómenos hidrometeorológicos y cambio climático, pp. 43-50, 2014.

[4] E. C. English, C. J. Friedland y F. Orooji, «Combined flood and wind mitigation for hurricane damage

prevention: case for amphibious construction,» Journal of Structural Engineering, 2017.

[5] N. Abdelfatah, A. Elawady, P. Irwin y A. G. Chowdhury, «Experimental investigation of wind impact on low-rise elevated residences,» Engineering Structures, vol. 257, pp. 096-114, 2022.

[6] M. Amini y A. M. Memari, «CFD-Based evaluation of elevated coastal residential buildings under hurricane wind loads,» Journal of Architectural Engineering, 2021.

[7] J. Holmes, «Wind pressures on tropical housing,» Wind Engineering and Industrial Aerodynamics , pp. 105-123, 1994.

[8] F. Xing , D. Mohotti y K. Chauhan, «Study on localised wind pressure developed in gable roof buildings having different roof pitches with experiments, RANS and LES simulation models,» Building and Environment , vol. 143, pp. 240-257, 2018.

[9] J. Singh y A. K. Roy, «Effects of roof slope and wind direction on wind pressure distribution on the roof of a square plan pyramidal low-rise building using CFD simulation,» International Journal of Advanced Structural Engineering (, pp. 231-254, 2019.

[10] A. M. Aly, C. Chokwitthaya y R. Poche, «Retrofitting building roofs with aerodynamic features and solar panels to reduce hurricane damage and enhance eco-friendly energy production,» Sustainable Cities and Society, pp. 581-593, 2017.

[11] A.-M. Aly, «Aerodynamic mitigation of wind uplift loads on low-rise buildings,» Advantances in civil, enviromental, and materials researchs, 2014.

[12] N. Gaur y R. Raj, «Aerodynamic mitigation by corner modification on squere model under wind loads employing CFD and wind tunnel,» Ain Shams Engineering, 2020.

[13] Y. Tominaga, A. Mochida, R. Yoshie, H. Kataoka, T. Nozu, M. Yoshikawa y T. Shirasawa, «AIJ guidelines for practical applications of CFD to pedestrian wind environment around buildings,» Wind Engineering, pp. 1749-1761, 2008.

[14] J. Van Dormaal y G. Raithby, «Enhanced of the SIMPLE method for predicting incompressible fluid flows,» Numerical heat transfer, vol. 7, pp. 147-163, 1984.

[15] D. Hargreaves y N. Wright, Wind Engineering and Industrial Aerodynamics 95, pp. 335-369, 2007.

[16] K. Zore, G. Parkhi, B. Sasanapuri y A. Varghese, «ANSYS mosaic Poly-Hexacore mesh for high-lift aircraft configuration,» de 21th Annual CFD Symposium, Bangalore, 2019.